Computational Materials Science 207 (2022) 111273

Contents lists available at ScienceDirect

Computational Materials Science

journal homepage: www.elsevier.com/locate/commatsci

Full length article

First-principles study of radiation defects in silicon

Vladislav Pelenitsyn *, Pavel Korotaev

Dukhov Automatics Research Institute (VNIIA), Moscow 127055, Russia

ARTICLE INFO

Keywords:
Radiation defects
Defect formation energy
Charge transition level
Silicon
Density functional theory

ABSTRACT

The study of the properties of defects in silicon forming under irradiation condition has been carried out for many years, however, many open questions remain. Particularly, there are not comprehensive results for variety of radiation centers calculated at the same level of theory. For example the previously calculated transition levels and formation energies show a large scatter. In this work, we focus on the important radiation-induced defect complexes in Si: double vacancy, vacancy-oxygen, vacancy-phosphorus. Additionally, the phosphorus–vacancy-oxygen complex was studied. Formation energy, charge transition levels and binding energy were calculated from first-principles using the hybrid exchange–correlation functional HSE06. Spin-polarized calculations and large supercells allows us to obtain charge transition levels which agree well with experimental measurements.

1. Introduction

Despite the variety of semiconductors available, Si has been the most affordable and widespread for many years. Due to the ubiquitous use of silicon semiconductors, there are application areas where they can be affected by irradiation. As a result, the energy transferred to the lattice can lead to breaking of interatomic bonds and displacement of atoms with the formation of point defects such as vacancies and interstitial atoms [1]. It is known that in Si these point defects are highly mobile and can form a complex with impurity atoms or with other intrinsic defects existing in the lattice [2–12]. Some of the important radiation-induced defect complexes (centers) in Si are the double vacancy [13,14], E-center (vacancy-phosphorus) [15–17], and A-center (vacancy-oxygen) [18]. These defects are electrically and optically active, therefore knowledge of their characteristics is necessary for technological applications [19].

Predicting the behavior of silicon electronics under irradiation conditions requires a detailed knowledge of radiation centers properties, such as formation energy and charge transition levels [20–22]. The formation energy determines the equilibrium concentration of defects in the material and their possibility to bind into complexes. Deep levels of radiation centers in the band gap directly affect the electronic properties of the material, since they are effective recombination centers. At the moment, the main powerful tool for predicting these properties is the density functional theory (DFT) based calculations [23].

Nevertheless, despite the progress in recent decades in studies of radiation centers in silicon by DFT calculations [24–42], many open questions remain. Various approaches show significant disagreement in the values of the formation energy and the charge transitions levels. One of the main reasons for the disagreement is the choice of the approximation for the exchange correlation (XC) functional. The traditional XC functionals such as the local-density approximations (LDA) and generalized gradient approximation (GGA) suffer from the so-called "band gap problem" [43]. For Si the band gap is almost half the experimental [44]. The correct value of the band gap is crucial for the correct description of the defect properties. The hybrid XC functionals are used to solve this problem, which include part of the exact exchange from the Hartree–Fock theory. It allows us to more correctly predict the band gap and lattice parameters of semiconductors [45]. In particular, there are a number of works in which radiation centers in Si were investigated by hybrid functional [37–42]. However, in these works different computational methods were used, so there is no comprehensive result for the various radiation centers at the same level of theory.

The aim of our work is to investigate radiation centers in Si at the same level of theory. We will consider the following defects: the vacancy (V_{Si}), the substitutional phosphorus (P_{Si}), the interstitial oxygen (O_i), the double vacancy ($V_{Si}V_{Si}$), the A-center ($V_{Si}O_i$), the E-center ($P_{Si}V_{Si}$). In addition, the vacancy-oxygen–phosphorus complex ($P_{Si}V_{Si}O_i$) will be investigated. In this study the range-separated Heyd–Scuseria–Ernzerhof hybrid functional HSE06 [46–48] and the supercell method are employed. We will compare our results with similar works and with experimental data. The charge transitions levels and binding energies evaluated in this work are in good agreement with experimental observations.

* Corresponding author.
E-mail addresses: pelenitsyn.vladislav@gmail.com (V. Pelenitsyn), pvl.korotaev@gmail.com (P. Korotaev).

https://doi.org/10.1016/j.commatsci.2022.111273
Received 25 November 2021; Received in revised form 27 January 2022; Accepted 10 February 2022
Available online 28 February 2022

2. Methods

2.1. Computational approach

First-principle calculations were performed using the DFT plane wave basis VASP code (version 5.4.4) [49,50]. The HSE06 hybrid functional with 25% of the Hartree–Fock exchange and the screening parameter $\mu = 0.2$ Å^{-1} was employed [46–48]. The local part of HSE06 is set by the generalized gradient functional PBE [51]. The HSE06 functional has proven itself for computing the properties of semiconductors, in particular for Si [45].

The cutoff energy of the plane wave basis for all calculations was 450 eV, which ensured the convergence of the total energy for all considered defects. To calculate the total energy, a cubic silicon supercell of 512 atoms (without defect) was used. The choice of supercell size is discussed in Section 2.3. A lattice constant of Si $a_0 = 5.437$ Å was used in calculations, which is obtained from an 8 atom-site conventional cubic cell. This calculated a lattice constant is very close to the experimental $a_0^{\text{exp}} = 5.431$ Å [52]. The calculated band gap is $E_g = 1.16$ eV, which is consistent with the experimentally zero-temperature gap $E_g^{\text{exp}} = 1.17$ eV [53]. Due to the high computational costs for hybrid functionals atomic environment for each defect was obtained with the PBE functional and a Γ-centered $3 \times 3 \times 3$ k-point mesh. For calculations of the supercell total energy by HSE06 a single Γ-point mesh was used.

2.2. Defect formation energy

The formation energy of a defect in the charge state q can be calculated as [20,21]

$$E_f^q = E_d^q - E_b - \sum_i n_i \mu_i + q(\mu_e + E_v) + E_{corr}^q, \quad (1)$$

where q is the charge of the supercell in units of elementary charge, E_b is the total energy of the defect-free supercell, E_d^q is the total energy of the same supercell with the defect in the charge state q. The quantity n_i represents the numbers of atoms of type i that are added (n_i>0) or removed (n_i<0) from the defective supercell and μ_i corresponds to their chemical potentials. The μ_e is the Fermi energy relative to the top of the valence band maximum (VBM) E_v. Finally, E_{corr}^q is the correction term due to the long-range Coulomb interaction of defect with its images. It was calculated E_{corr}^q according to the scheme of Freysoldt, Neugebauer, and Van de Walle [54,55]. The experimental dielectric constant $\varepsilon = 11.7$ [56] was used for correction term.

The charge transition energy level $\varepsilon(q_1/q_2)$ is defined as the Fermi energy at which the formation energies of charge states q_1 and q_2 of the defect are the same. These charge transition level can be found from Eq. (1) as

$$\varepsilon(q_1/q_2) = \frac{E_f^{q_1}(\mu_e = 0) - E_f^{q_2}(\mu_e = 0)}{q_2 - q_1}. \quad (2)$$

Above the transition level $\varepsilon(q_1/q_2)$ the charge state q_2 is stable and below the charge state q_1 is stable.

To investigate the tendency of the defects to form complexes it is useful to calculate the binding energy, which indicates the minimum energy required to separate the defect complex into non-interacting points defects. Binding energy E_b can be calculated as

$$E_b = \sum_i E_f(i) - E_f(C) \quad (3)$$

where $E_f(i)$ is the formation energy of the defect i, $E_f(C)$ is complex formation energy. Positive sign of the binding energy indicates a thermodynamically stable bound complex. Also it is possible to determine the binding energy of an one complex A with either another complex (or point defect) B

$$E_b(\text{A},\text{B}) = E_f(\text{A}) + E_f(\text{B}) - E_f(\text{AB}) \quad (4)$$

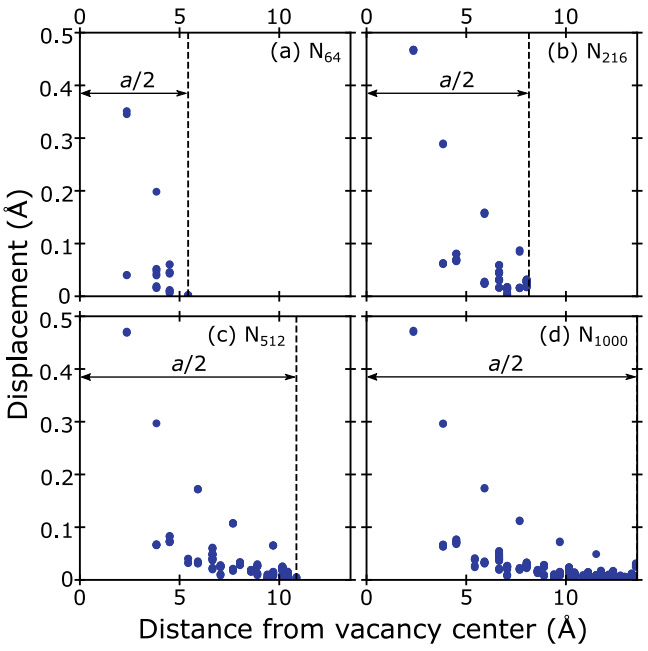

Fig. 1. Displacements of atoms after relaxation in the Si supercell of (a) 64-atom sites, (b) 216-atom sites, (c) 512-atom sites, (d) 1000-atom sites size as a function of the distance from the vacancy center in a perfect supercell. Displacements are plotted to the half the supercell's linear size $a/2$, where a - supercell's lattice parameter.

Note that the positiveness of E_b may be not sufficient to ensure the thermodynamic stability of a complex. The analysis of free energy and configurational entropy is required (a more detailed discussion in Section 2.F in Ref. [57]).

2.3. Supercell size

Defects and their complexes have the local atomic environment that can be quite different from an ideal lattice. The atomic environment must be optimized to correctly determine the characteristics of defects. However, the elastic interaction of atoms with their images can occur due to the periodic boundary conditions (PBC), giving a spurious contribution to the formation energy [22]. This contribution should be minimized as much as possible. One possible way is to increase the supercell size. The dependence of the formation energy from the supercell size had already been investigated, for example, for the single silicon vacancy in Si in Refs. [25,27,58–60]. In present work, we want to complement this researches by considering the dependence of atomic displacements after ionic relaxation on the supercell size. We investigated the case of neutral single vacancy in the supercells of 64-, 216-, 512-, 1000-atom sites.

The presence of a defect in a lattice can distort the local symmetry of a perfect crystal. To break the original symmetry, small random displacements were given to the atoms, followed by position optimization. The resulting structure does not depend on the initial random displacements.

The displacements of atoms after relaxation around the vacancy are shown in Fig. 1. It is clear the larger the cell, the less the displacements far from the vacancy. Negligible displacements far from defect mean that the interactions between periodic images of atoms through the PBC are minimized. The corresponding neutral vacancy formation energy obtained with the PBE functional after relaxation are $E_f^{64} = 3.54$ eV, $E_f^{216} = 3.38$ eV, $E_f^{512} = 3.34$ eV and $E_f^{1000} = 3.33$ eV. The choice of a large supercell size makes it possible to reduce the effect of PBC on the formation energy. Supercells of 64 and 216 atoms introduce an error from tens to hundreds meV. In further calculations (taking into account

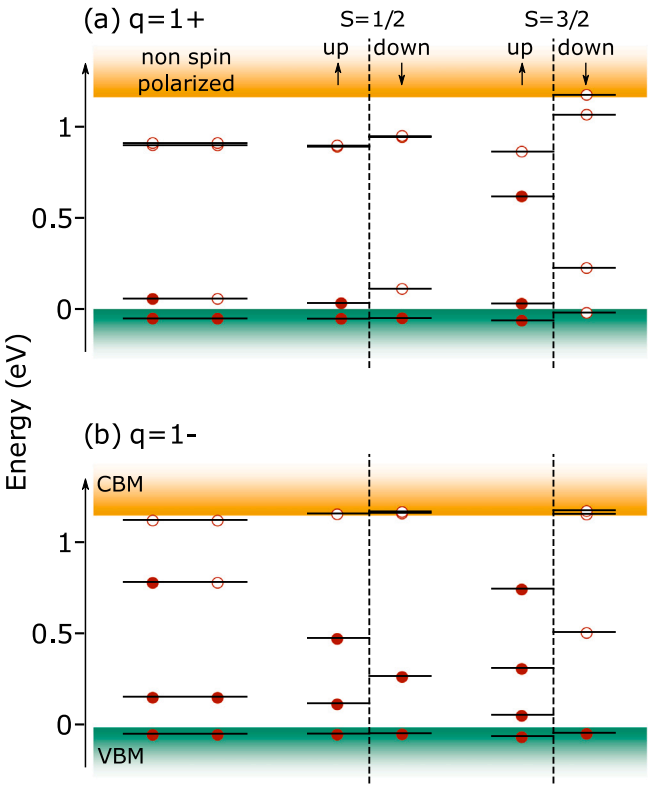

Fig. 2. Vacancy single-particle levels at the Γ-point of (a) V_{Si}^{1+}, (b) V_{Si}^{1-} charge states. For each charge state, the defect single-particle levels are shown for the non spin-polarized case and with total spin moment $S = 1/2$ and $S = 3/2$ cases. The occupied levels are plotted with filled circles, empty levels with open circles.

the possible error about 0.01 eV) we will focus on a supercell of 512-atom due to the high computational costs for a larger cells, especially when using the hybrid functional.

Note in the case of a charged defects there is also a spurious electrostatic interaction between periodic images due to PBC. It is corrected via Freysoldt–Neugebauer–Van de Walle (FNV) scheme and a large supercell should be used to calculate correction term accurately. An example of using the FNV scheme for supercells of different size for the charged vacancy is presented in the Supplemental Material, Fig. S1. A large supercell allows us to minimize a spurious elastic and electrostatic interactions between defect images.

2.4. Influence of the spin degree of freedom

The ground state of a defect with localized deep levels occupied by electrons can have nonzero spin moment. Therefore the spin degrees of freedom should be taken into account for accurate formation energy calculation. In order to show this the spin polarized calculations for the single vacancy were performed.

We focused on the electronic structure of the 1+ and 1− charge states. Electronic configurations of the doublet ($S = 1/2$) and the quartet ($S = 3/2$) states were considered. The single-particle Kohn–Sham levels associated with the vacancy at Γ-point for the different spin states are shown in Fig. 2. The significant change for the position of the electronic levels is observed in the case of spin-polarized calculations. In general the filled levels has got closer to the conduction band. Also the doublet and the quartet electronic configurations highly differ from each other. The change in the position of the electronic levels for charge states increase with the increasing of the total spin moment.

The change in the total energy leads to a change in the value of the charge transition level (Eq. (2)). For the vacancy the formation energies

Table 1
Formation energy E_f^0, binding energy E_b calculated for the neutral considered defects in Si (This work), along with the previously reported results (Other work), which are obtained using hybrid XC functional.

Defect	E_f^0 (eV)		E_b (eV)
	This work	Other work	This work
V_{Si}	4.14	4.08[a]	
		4.30[b]	
		4.19[c]	
		4.58[d]	
		3.38[e]	
$V_{Si}V_{Si}$	6.31	4.79[e]	1.97
		6.64[f]	
		6.08[c]	
O_i	1.70	1.95[d]	
$V_{Si}O_i$	3.95	5.20[e]	1.89
		4.30[d]	
P_{Si}	0.37		
$V_{Si}P_{Si}$	2.95	3.40[g]	1.56
$P_{Si}V_{Si}O_i$	2.80	3.08[g]	3.41

[a]Ref. [44]
[b]Ref. [41]
[c]Ref. [39]
[d]Ref. [40]
[e]Ref. [37]
[f]Ref. [38]
[g]Ref. [42]

in the most stable states lower than in the non spin polarized cases by −0.09, −0.04, −0.03, −0.22, −0.02 eV for the charges from 2+ to 2− respectively. Thus for instance, the change in $\epsilon(0/1-)$ transition level will be 0.19 eV (Eq. (2)). This change is significant for the position of the transition level within the silicon band gap (1.16 eV from HSE06 calculation).

To determine the energetically favorable spin states, calculations were carried out for all considered defects with various total spin moments. For all the cases the configurations with the lowest possible total spin moments are the most stable. Accordingly, for odd charge states it is doublet ($S = 1/2$), and for even it is singlet ($S = 0$). In what follows we will only consider these configurations.

3. Results and discussion

The calculated formation energy of the considered defects in neutral charge state at Fermi level $\mu_e = 0$ (Eq. (1)) and the complexes binding energy (Eq. (4)) along with other published results are presented in Table 1. For comparison with the previous DFT results, the studies that used the hybrid HSE functional were selected. The choice of the correction scheme for charged state calculations can greatly affect the formation energy. Therefore, we compared only the neutral charge defects. The formation energy for charged states at $\mu_e = 0$ are presented in Supplemental Material in Table T1. The formation energy as a function of the Fermi level for the considered defects are shown in Fig. 3(a)–(f). The calculated charge transition levels (Eq. (2)) are shown in Figure Fig. 3(g) and Table 2. The previous published results and the experimental data are also presented in Table 2. Further, we will discuss the obtained results for each defect.

3.1. Vacancy and double vacancy

While single and double vacancy in silicon are well studied, here we provide our results to benchmark current method.

The optimized structures for positive and neutral charge states of V_{Si} are in agreement with the electron paramagnetic resonance (EPR) experimental observations and Watkins' linear-combination-of-atomic-orbitals (LCAO) model [19]: D_{2d} point group symmetry for V_{Si}^{1+} and V_{Si}^{0}, T_d for V_{Si}^{2+}. For double negative vacancy V_{Si}^{2-} the obtained configuration

Table 2
Charge transition levels $\varepsilon(q_1/q_2)$ calculated for the considered defects in Si (This work), along with the previously reported results (Other works) and the experimental data (Expt.). All values are presented in (eV) relative to E_v. An asterisk (*) means that the acceptor level is recalculated to the distance from the VBM, assuming the experimental room-temperature band gap of 1.12 eV [53].

Transition	V_{Si}			$V_{Si}V_{Si}$			$V_{Si}O_i$			$P_{Si}V_{Si}$			$P_{Si}V_{Si}O_i$	
level	This work	Other works	Expt.[a]	This work	Other work[b]	Expt.[c]	This work	Other works	Expt.[d]	This work	Other work[e]	Expt.[f]	This work	Other work[e]
$\varepsilon(2+/1+)$	0.13	0.14[g]	0.13	−0.14	0.09		−0.14			−0.01			−0.15	
$\varepsilon(2+/0)$	0.09	0.08[g] 0.04[h]	0.09	0.03			−0.09			−0.12			0.03	
$\varepsilon(1+/0)$	0.05	0.02[g]	0.04	0.20	0.62	0.21	−0.03			0.19	0.16	0.27	0.22	0.17
$\varepsilon(0/1-)$	0.70	1.05[g] 0.33[h] 0.35[b]	<1.00	0.64	0.64	0.72*	0.92	0.54[h] 0.83[b]	0.95*	0.76	0.17	0.67*	0.96	0.69
$\varepsilon(0/2-)$	0.77	0.91[g] 0.27[h]		0.77			1.17	0.54[h]		1.05	0.21		1.16	0.85
$\varepsilon(1-/2-)$	0.88	0.77[g] 0.21[h] 0.65[b]	<1.00	0.92	0.80	0.89*	1.42	0.53[h] 0.94[b]		1.32	0.24		1.36	1.02

[a]Refs. [19,61]
[b]Ref. [37]
[c]Refs. [13,62]
[d]Ref. [18]
[e]Ref. [42]
[f]Ref. [16,63]
[g]Ref. [44]
[h]Ref. [40]

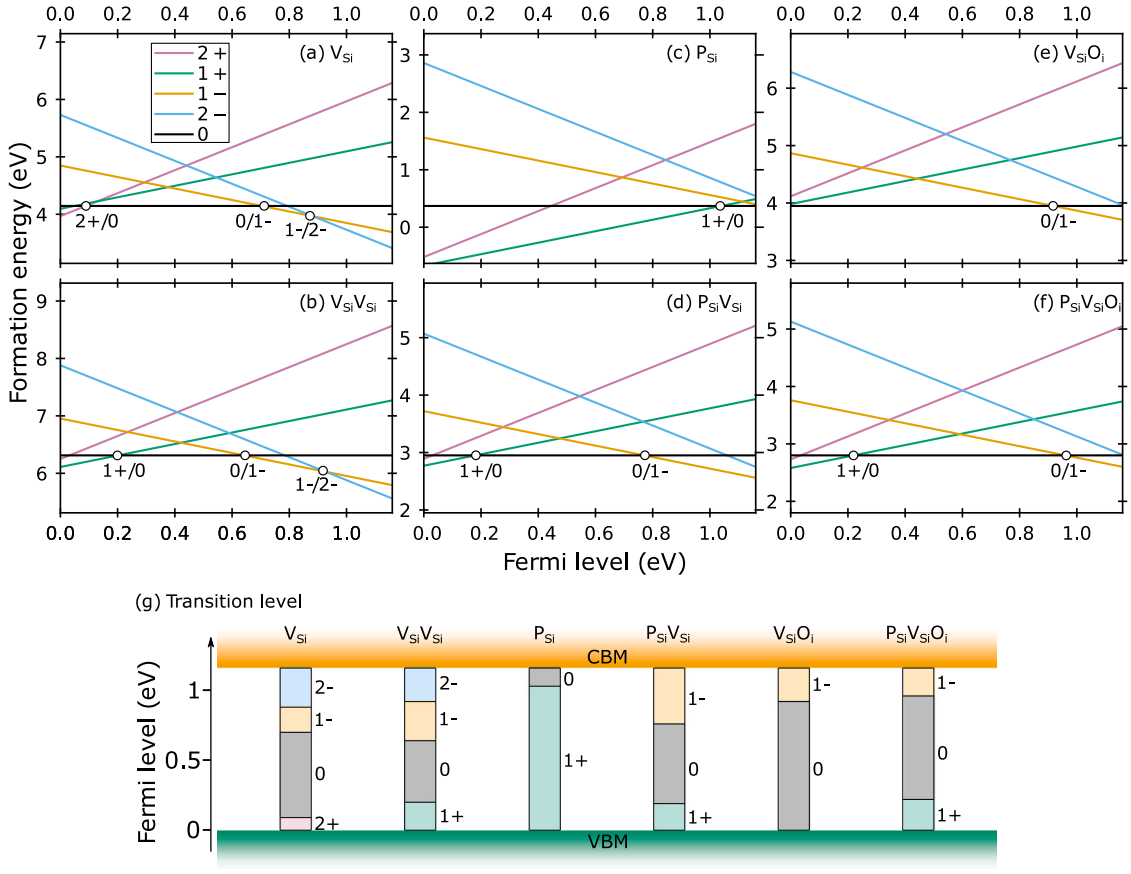

Fig. 3. The formation energy as a function of the Fermi energy of (a) V_{Si}, (b) $V_{Si}V_{Si}$, (c) P_{Si}, (d) $P_{Si}V_{Si}$, (e) $V_{Si}O_i$, (f) $P_{Si}V_{Si}O_i$. The positions of the charge transition levels are plotted with circles. Note that P_{Si} is shallow donor, and its formation energy and transition level are only an estimate of their location. (g) Charge transition levels of the considered defects.

is 'split vacancy' with a point group D_{3d} in also agreement with previous theoretical studies [24,44,58–60]. For negative charge state V_{Si}^{1-} we found the atomic configuration with symmetry close to experimentally observed C_{2v} [64,65] with deviations of about 0.07 Å.

The obtained atomic structures of a double vacancy are a resonant-bond configuration (*RB*) (see Fig. 4) with C_{2h} symmetry, excluding the case of double positive charge state, which was found in S_2 low symmetry ($d_{12} \neq d_{13} \neq d_{23}$, see Fig. 4). According to the LCAO model

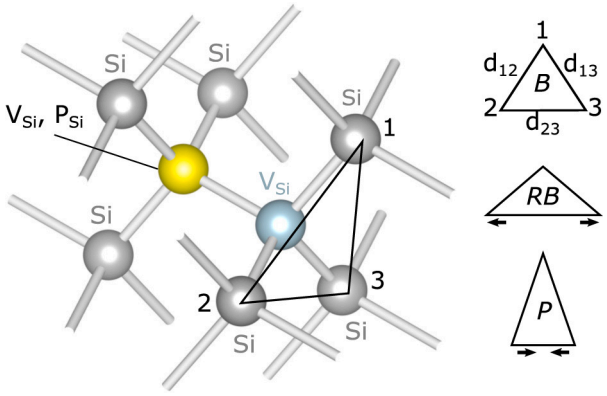

Fig. 4. Schematic local structure of $V_{Si}V_{Si}$ and $P_{Si}V_{Si}$ in Si. There are three possible configurations: breathing mode (B) configuration ($d_{12} = d_{13} = d_{23}$, resonant bond (RB) structure ($d_{12} = d_{13} < d_{23}$), pairing (P) configuration ($d_{12} = d_{13} > d_{23}$). For $V_{Si}V_{Si}$ the configuration is symmetric with respect to each vacancy.

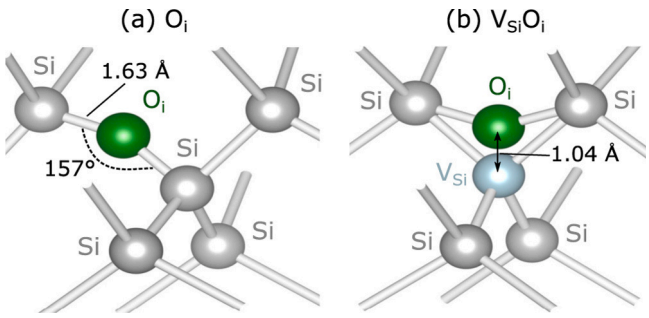

Fig. 5. Local structure of (a) O_i, (b) $V_{Si}O_i$ in Si. O_i forms a bond Si-O_i-Si with an angle 157° and O_i-Si bonds length of 1.63 Å. In the local structure of V_{SiO_i} the oxygen atom is displaced from the vacancy center by a distance 1.04 Å.

and EPR experiments by Watkins and Corbett [14,66] both the single charged $V_{Si}V_{Si}$ (+ and −) has a pairing configuration (P) with C_{2h} symmetry. However, the calculated total energy difference between the configurations of $V_{Si}V_{Si}$ is less than 30 meV, that weakly affected on E_f. In the previous DFT studies (Refs. [25–27]) the maximum difference in the total energies between the $V_{Si}V_{Si}$ configurations was about 40 meV.

The calculated formation energies for neutral charge state $E_f(V^0_{Si}) =$ 4.14 eV and $E_f(V_{Si}V^0_{Si}) = 6.31$ eV in general are similar to the previous HSE XC functional studies; see Table 1 and Fig. 3(a)–(b). Śpiewak and Kurzydłowski [44] used the same supercell size for single vacancy calculation, and their formation energy $E_f(V^0_{Si}) = 4.08$ eV is very close to result in this work. The reasons for differences with other results may be the smaller supercell size (Refs. [37–41]), the use of norm-conserving pseudopotential (Ref. [37]). Also, in the previous works the spin degree of freedom has not been taken into account. As discussed in Section 2, supercell size and spin polarization can strongly affect the formation energy.

The charge transition level (Table 2) are in good agreement with the experimentally measured. For a single vacancy the "negative-U" effect [67,68] is also observed: the transition occurs directly from V^{2+}_{Si} to V^0_{Si} at the transition level $\varepsilon(2+/0) = 0.09$ eV, the single positive charge state V^{1+}_{Si} is unstable. In contrast to the vacancy donor levels there is no well established experimental values for the acceptor levels. Is was suggested from the results of the deep-level transient spectroscopy (DLTS) that they are located at more than about 0.17 eV below the conduction band minimum [68]. Also, several other experiments [61,69,70] confirm the existence of the vacancy acceptor levels. The calculated values $\varepsilon(0/1-) = 0.7$ eV and $\varepsilon(1-/2-) = 0.88$ eV and the previous hybrid functional results (Table 2) corroborate experimental findings. For a double vacancy the calculated transition levels are in excellent agreement with the DLTS experimental data [13,62].

Comparison with previous hybrid functional studies (Table 2) shows a large scatter in the calculated transition energies. The calculated donor levels of V_{Si} are generally similar, but for the acceptor levels the difference is stronger. As we already pointed out a variance may arise due to different computational parameters for the formation energy calculation. Also in Refs. [37,44] different schemes for calculating the correction term were used. For the $V_{Si}V_{Si}$ only the acceptor level $\varepsilon(0/1-)$ coincides with Ref. [37], but for other levels there is a great discrepancy.

The calculated binding energy for the double vacancy $E_b(V_{Si}V_{Si}) =$ 1.97 eV (Table 1) agrees with the experimental estimated value of ≥ 1.6 eV [26].

3.2. A-center

The local atomic structure of interstitial oxygen after supercell relaxation is shown in Fig Fig. 5(a). The oxygen atom displaced off from bond-centered position and form Si-O_i-Si configuration with an angle 157° and O_i-Si bonds length of 1.63 Å. It is consistent with the previous predicted structure of O_i by Pesola et al. [28] and general accepted model for O_i [71,72]. Also the value of a bond angle 157° is in good agreement with the experimental one of 162° [71].

We distinguished only the neutral charge state of O_i to be stable within the band gap. The calculated formation energy $E_f(O^0_i) =$1.7 eV (Table 1) is less than the value of 1.95 eV calculated by Wang et al. using a smaller supercell with 64-atom sites [40]. They also observed that O_i only has a neutral stable charge state in the band gap.

The obtained atomic local structure of $V_{Si}O_i$ complex after relaxation is shown in Fig. Fig. 5(b). The oxygen atom occupies a position displaced from the vacancy center by 1.04 Å between two silicon atoms forming the Si-O_i-Si bond. The point group symmetry is C_{2v} agrees with the EPR measurements by Watkins and Corbett [18] and the previous studies [28–31,73]. We also found another configuration with displacement length of 0.3 Å. However, this configuration is less energy favored by 0.02 eV.

The chemical potential of an oxygen atom μ_O was calculated using low-temperature form of SiO_2, α-quartz, as $\mu_O = (E_{tot}(SiO_2) - 3\mu_{Si})/6$, where $E_{tot}(SiO_2)$ is the total energy of the SiO_2.

The formation energies as a function of the position of the Fermi level for the charged states of A-center are shown in Fig. 3(e). The A-center has an only acceptor level $\varepsilon(0/1-) = 0.92$ eV in the band gap. This closely agrees with the experimental observations and measured value for this level of 0.95 eV by Watkins and Corbett [18]. In contrast to the previous hybrid DFT studies [37,40] (Table 2) we did not obtain other acceptor levels in the band gap.

The calculated formation energy of the neutral A-center is $E_f(V_{Si}O^0_i) = 3.95$ eV (Table 1). It is, however, less than the calculated values from Refs. [37,40] (Table 1). The possible reasons for the discrepancies were discussed earlier. The calculated binding energy $E_b(V_{Si}O_i) = 1.89$ eV (Table 1) also agrees with the experimentally measured value of 1.94 eV [32].

3.3. E-center

Let us consider a phosphorus substitutional dopant P_{Si} first. It is well known that P_{Si} is a shallow donor with a "hydrogenic" state, the wavefunction of which is relatively delocalized. The calculations of P_{Si} transition levels by the presented methods (Section 2) could not be reliable and require a much larger supercell. Therefore, for P_{Si} we will only estimate their location in the band gap.

The chemical potential of the phosphorus μ_P was calculated using the black phosphorus conventional cell, containing 4 atoms, as $\mu_P =$

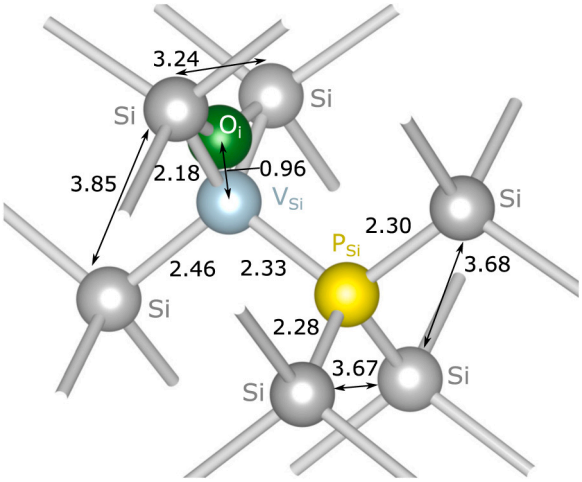

Fig. 6. Local structure of $P_{Si}V_{Si}O_i$ in Si. Distances between the defects and the neighboring Si atoms are shown in units of Å.

$\frac{1}{4}E_{tot}$(P), where E_{tot}(P) is the total energy of black P. The calculated formation energy of P_{Si} as a function of the Fermi energy is shown in Fig. 3(c). As expected [7,15] P_{Si} act as a shallow donor with the transition level located near conduction-band minimum (CBM). The calculated value is 0.13 eV from CBM, which is larger than the experimentally established of 0.045 eV [15].

E-center was obtained after atomic position optimization with C_{2h} symmetry in a *P* configuration (Fig. 4) for neutral charge state and an *RB* configuration for negative states, which is consistent with experimental data [17,74]. Positively charged states were found in an breathing mode (*BM*) configuration with D_{3d} symmetry, in agreement with the previous theoretical studies [35,75].

As shown in Fig. 3(d) and Fig. 3(g), $P_{Si}V_{Si}$ has both deep acceptor $\varepsilon(0/1-)$ and donor $\varepsilon(+/0)$ levels. The donor level $\varepsilon(+/0)$ was observed only recently by minority-carrier transient spectroscopy experiment, and our calculated value of 0.19 eV (Table 2) is close to the experimental one 0.27 eV [63]. The calculated acceptor level $\varepsilon(0/-) = 0.76$ eV is also close to the experimental value of 0.67 eV [16]. The previous hybrid functional DFT study (Ref. [42]) also confirms existence of donor level with energy of 0.16 eV, however the result for donor level of 0.17 eV is much lower.

The experimental values of the E-center binding energy are in the range of 0.55–1.87 eV [3–6,17,76–78]. The reason for this scatter lies in different assumptions about phosphorus diffusion. The calculated binding energy $E_b(P_{Si}V_{Si}) = 1.56$ eV falls within the range of experimental values.

3.4. Phosphorous–vacancy-oxygen complex

The $P_{Si}V_{Si}O_i$ complex can be formed in consequence of the interaction of either the A-center with substitutional phosphorus ($V_{Si}O_i + P_{Si} \rightarrow P_{Si}V_{Si}O_i$), or the E-center with interstitial oxygen ($P_{Si}V_{Si} + O_i \rightarrow P_{Si}V_{Si}O_i$). To find the atomic structure of the $P_{Si}V_{Si}O_i$, we considered separately both cases. All possible initial positions of phosphorus and oxygen atoms from the corresponding complexes up to the third nearest neighbor silicon atom were considered. As a result, the same structure of the $P_{Si}V_{Si}O_i$ (Fig. 6) complex with C_{2h} symmetry was obtained after atomic positions optimization to be the most energetically favorable in both cases. A similar structure was also discussed in Refs. [36,42] as a more stable configuration.

Fig. 3(f)–(g) show the formation energy of $P_{Si}V_{Si}O_i$ in various charge states as a function of μ_e. $P_{Si}V_{Si}O_i$ has acceptor $\varepsilon(0/1-) = 0.96$ eV and donor $\varepsilon(1 + /0) = 0.22$ eV deep levels. Since the $P_{Si}V_{Si}$ complex has only deep levels and low formation energy (see Table 1) like the previously considered radiation centers, it might be an effective recombination center for Si. As in the case $P_{Si}V_{Si}$, our calculated transition levels differ from the values of Ref. [42] (Table 2) and we also did not found the $\varepsilon(-/2-)$ acceptor level to be located in the band gap.

The binding energy of $P_{Si}V_{Si}O_i$ is 3.41 eV. We also calculated the binding energies for the above considered interaction to form $P_{Si}V_{Si}O_i^0$: $E_b(V_{Si}O_i + P_{Si}) = 1.52$ eV and $E_b(V_{Si}P_{Si} + O_i) = 1.85$ eV. Note that the defects are assumed to be charge neutral. The differences in binding energies indicate that in neutral charge states interaction between E-center and oxygen interstitial atom is more attractive than between A-center and substitutional phosphorus. A high binding energy assumes that, in principle, the $P_{Si}V_{Si}O_i$ complex could be formed in Si by this interaction. However, as mentioned in Section 2.2 in order to calculate the equilibrium concentration it is necessary to investigate its configurational entropy.

4. Conclusion

In this work, we presented the formation energies, binding energies and charge transition levels of the radiation centers and defects in silicon at the same level of theory using the HSE06 hybrid functional. We used the supercell approach (within 512 atoms), taking into account a spin degree of freedom and finite-size electrostatic corrections (FNV scheme). We showed that this methods allow us to obtain the charge transition levels and binding energies, which are in a good agreement with the experimental data.

On other hand, comparison with the results from previous DFT studies using the hybrid functional showed a large scatter in the calculated values of the charge transition levels. This means that in addition to the choice of the XC functional, the result is strongly influenced by other calculation parameters, such as the supercell size, the pseudopotential, and the choice of the scheme for finite-size correction. We believe that the methods used in this work for the radiation centers investigation can be applied to simulate radiation damage in silicon.

CRediT authorship contribution statement

Vladislav Pelenitsyn: Conceptualization, Methodology, Formal analysis, Investigation, Writing – original draft. **Pavel Korotaev:** Conceptualization, Writing – review & editing, Supervision, Project administration.

Declaration of competing interest

The authors declare that they have no known competing financial interests or personal relationships that could have appeared to influence the work reported in this paper.

Data availability

The data that support the findings of this study are available from the corresponding author upon reasonable request.

Appendix A. Supplementary data

Supplementary material related to this article can be found online at https://doi.org/10.1016/j.commatsci.2022.111273.

References

[1] C. Claeys, E. Simoen, Basic radiation damage mechanisms in semiconductor materials and devices, in: Radiation Effects in Advanced Semiconductor Materials and Devices, Springer Berlin Heidelberg, Berlin, Heidelberg, 2002, pp. 9–52, http://dx.doi.org/10.1007/978-3-662-04974-7_2.

[2] R. Car, P.J. Kelly, A. Oshiyama, S.T. Pantelides, Microscopic theory of impurity-defect reactions and impurity diffusion in silicon, Phys. Rev. Lett. 54 (4) (1985) 360–363, http://dx.doi.org/10.1103/PhysRevLett.54.360.

[3] D. Shaw, Self- and impurity diffusion in Ge and Si, Phys. Status Solidi (B) 72 (1) (1975) 11–39, http://dx.doi.org/10.1002/pssb.2220720102.

[4] R.B. Fair, J.C.C. Tsai, A quantitative model for the diffusion of phosphorus in silicon and the emitter dip effect, J. Electrochem. Soc. 124 (7) (1977) 1107, http://dx.doi.org/10.1149/1.2133492.

[5] M. Yoshida, Diffusion of group V impurity in silicon, Japan. J. Appl. Phys. 10 (6) (1971) 702–713, http://dx.doi.org/10.1143/jjap.10.702.

[6] M. Hirata, M. Hirata, H. Saito, The interactions of point defects with impurities in silicon, J. Phys. Soc. Japan 27 (2) (1969) 405–414, http://dx.doi.org/10.1143/JPSJ.27.405.

[7] P. Pichler, Dopants, in: Intrinsic Point Defects, Impurities, and their Diffusion in Silicon, Springer Vienna, Vienna, 2004, pp. 331–467, http://dx.doi.org/10.1007/978-3-7091-0597-9_5.

[8] C.A. Londos, N. Sarlis, L.G. Fytros, K. Papastergiou, Precursor defect to the vacancy-dioxygen center in Si, Phys. Rev. B 53 (1996) 6900–6903, http://dx.doi.org/10.1103/PhysRevB.53.6900.

[9] N.V. Sarlis, C.A. Londos, L.G. Fytros, Origin of infrared bands in neutron-irradiated silicon, J. Appl. Phys. 81 (4) (1997) 1645–1650, http://dx.doi.org/10.1063/1.364020.

[10] V.P. Markevich, A.R. Peaker, S.B. Lastovskii, L.I. Murin, J. Coutinho, V.J.B. Torres, P.R. Briddon, L. Dobaczewski, E.V. Monakhov, B.G. Svensson, Trivacancy and trivacancy-oxygen complexes in silicon: Experiments and ab initio modeling, Phys. Rev. B 80 (2009) 235207, http://dx.doi.org/10.1103/PhysRevB.80.235207.

[11] V.P. Markevich, A.R. Peaker, B. Hamilton, S. Lastovskii, L.I. Murin, J. Coutinho, M.J. Rayson, P.R. Briddon, B.G. Svensson, The trivacancy and trivacancy-oxygen family of defects in silicon, in: Gettering and Defect Engineering in Semiconductor Technology XV, in: Solid State Phenomena, vol. 205, Trans Tech Publications Ltd, 2014, pp. 181–190, http://dx.doi.org/10.4028/www.scientific.net/SSP.205-206.181.

[12] E.A. Tolkacheva, V.P. Markevich, L.I. Murin, Optical properties and the mechanism of the formation of V_2O_2 and V_3O_2 vacancy–oxygen complexes in irradiated silicon crystals, Semiconductors 52 (9) (2018) 1097–1103, http://dx.doi.org/10.1134/S1063782618090221.

[13] B.G. Svensson, B. Mohadjeri, A. Hallén, J.H. Svensson, J.W. Corbett, Divacancy acceptor levels in ion-irradiated silicon, Phys. Rev. B 43 (3) (1991) 2292–2298, http://dx.doi.org/10.1103/PhysRevB.43.2292.

[14] G.D. Watkins, J.W. Corbett, Defects in irradiated silicon: Electron paramagnetic resonance of the divacancy, Phys. Rev. 138 (1965) A543–A555, http://dx.doi.org/10.1103/PhysRev.138.A543.

[15] G.L. Pearson, J. Bardeen, Electrical properties of pure silicon and silicon alloys containing boron and phosphorus, Phys. Rev. 75 (5) (1949) 865–883, http://dx.doi.org/10.1103/PhysRev.75.865.

[16] A. Chantre, M. Kechouane, D. Bois, Vacancy-diffusion model for quenched-in E-centers in CW laser annealed virgin silicon, Physica B+C 116 (1) (1983) 547–552, http://dx.doi.org/10.1016/0378-4363(83)90305-4.

[17] G.D. Watkins, J.W. Corbett, Defects in irradiated silicon: electron paramagnetic resonance and electron-nuclear double resonance of the Si-E center, Phys. Rev. 134 (5A) (1964) A1359–A1377, http://dx.doi.org/10.1103/PhysRev.134.A1359.

[18] G.D. Watkins, J.W. Corbett, Defects in irradiated silicon. I. electron spin resonance of the Si-A center, Phys. Rev. 121 (4) (1961) 1001–1014, http://dx.doi.org/10.1103/PhysRev.121.1001.

[19] G.D. Watkins, Intrinsic defects in silicon, Mater. Sci. Semicond. Process. 3 (4) (2000) 227–235, http://dx.doi.org/10.1016/S1369-8001(00)00037-8.

[20] S.B. Zhang, J.E. Northrup, Chemical potential dependence of defect formation energies in GaAs: Application to Ga self-diffusion, Phys. Rev. Lett. 67 (1991) 2339–2342, http://dx.doi.org/10.1103/PhysRevLett.67.2339.

[21] C.G. Van de Walle, D.B. Laks, G.F. Neumark, S.T. Pantelides, First-principles calculations of solubilities and doping limits: Li, Na, and N in Znse, Phys. Rev. B 47 (1993) 9425–9434, http://dx.doi.org/10.1103/PhysRevB.47.9425.

[22] C. Freysoldt, B. Grabowski, T. Hickel, J. Neugebauer, G. Kresse, A. Janotti, C.G. Van de Walle, First-principles calculations for point defects in solids, Rev. Modern Phys. 86 (1) (2014) 253–305, http://dx.doi.org/10.1103/RevModPhys.86.253.

[23] P. Hohenberg, W. Kohn, Inhomogeneous electron gas, Phys. Rev. 136 (1964) B864–B871, http://dx.doi.org/10.1103/PhysRev.136.B864.

[24] M.G. Ganchenkova, L.E. Oikkonen, V.A. Borodin, S. Nicolaysen, R.M. Nieminen, Vacancies and E-centers in silicon as multi-symmetry defects, Mater. Sci. Eng. B 159–160 (2009) 107–111, http://dx.doi.org/10.1016/j.mseb.2008.10.040.

[25] J. Dabrowski, G. Kissinger, Supercell-size convergence of formation energies and gap levels of vacancy complexes in crystalline silicon in density functional theory calculations, Phys. Rev. B 92 (14) (2015) 144104, http://dx.doi.org/10.1103/PhysRevB.92.144104.

[26] M. Pesola, J. von Boehm, S. Pöykkö, R.M. Nieminen, Spin-density study of the silicon divacancy, Phys. Rev. B 58 (3) (1998) 1106–1109, http://dx.doi.org/10.1103/PhysRevB.58.1106.

[27] R.R. Wixom, A.F. Wright, Formation energies, binding energies, structure, and electronic transitions of Si divacancies studied by density functional calculations, Phys. Rev. B 74 (20) (2006) 205208, http://dx.doi.org/10.1103/PhysRevB.74.205208.

[28] M. Pesola, J. von Boehm, T. Mattila, R.M. Nieminen, Computational study of interstitial oxygen and vacancy-oxygen complexes in silicon, Phys. Rev. B 60 (16) (1999) 11449–11463, http://dx.doi.org/10.1103/PhysRevB.60.11449.

[29] A. Chroneos, C.A. Londos, Interaction of A-centers with isovalent impurities in silicon, J. Appl. Phys. 107 (9) (2010) 093518, http://dx.doi.org/10.1063/1.3409888.

[30] R.A. Casali, H. Rücker, M. Methfessel, Interaction of vacancies with interstitial oxygen in silicon, Appl. Phys. Lett. 78 (7) (2001) 913–915, http://dx.doi.org/10.1063/1.1347014, Publisher: American Institute of Physics.

[31] C.A. Londos, E.N. Sgourou, D. Hall, A. Chroneos, Vacancy-oxygen defects in silicon: the impact of isovalent doping, J. Mater. Sci., Mater. Electron. 25 (6) (2014) 2395–2410, http://dx.doi.org/10.1007/s10854-014-1947-6.

[32] N.I. Boyarkina, S.A. Smagulova, A.A. Artem'ev, Dissociation energies of a CiCs complex and the A center in silicon, Semiconductors 36 (8) (2002) 845–847, http://dx.doi.org/10.1134/1.1500457.

[33] R. Virkkunen, R.M. Nieminen, First-principles study of the phosphorous-vacancy pair in silicon, Comput. Mater. Sci. 1 (4) (1993) 351–357, http://dx.doi.org/10.1016/0927-0256(93)90031-H.

[34] M.G. Ganchenkova, A.Y. Kuznetsov, R.M. Nieminen, Electronic structure of the phosphorus-vacancy complex in silicon: A resonant-bond model, Phys. Rev. B 70 (11) (2004) 115204, http://dx.doi.org/10.1103/PhysRevB.70.115204.

[35] G. Herrero-Saboya, L. Martin-Samos, A. Jay, A. Hemeryck, N. Richard, A comprehensive theoretical picture of e centers in silicon: From optical properties to vacancy-mediated dopant diffusion, J. Appl. Phys. 127 (8) (2020) 085703, http://dx.doi.org/10.1063/1.5140724.

[36] A. Chroneos, E.N. Sgourou, C.A. Londos, Interaction of n-type dopants with oxygen in silicon and germanium, J. Appl. Phys. 112 (7) (2012) 073706, http://dx.doi.org/10.1063/1.4757406.

[37] A. Abdurrazaq, A.T. Raji, W.E. Meyer, Effect of isovalent doping on hydrogen passivated vacancy-oxygen defect complexes in silicon: Insights from density functional theory, Silicon (2020) http://dx.doi.org/10.1007/s12633-020-00548-5.

[38] S.-R.G. Christopoulos, H. Wang, A. Chroneos, C.A. Londos, E.N. Sgourou, U. Schwingenschlögl, VV and VO2 defects in silicon studied with hybrid density functional theory, J. Mater. Sci., Mater. Electron. 26 (3) (2015) 1568–1571, http://dx.doi.org/10.1007/s10854-014-2576-9.

[39] W. Gao, A. Tkatchenko, Electronic structure and van der waals interactions in the stability and mobility of point defects in semiconductors, Phys. Rev. Lett. 111 (2013) 045501, http://dx.doi.org/10.1103/PhysRevLett.111.045501.

[40] H. Wang, A. Chroneos, C.A. Londos, E.N. Sgourou, U. Schwingenschlögl, A-centers in silicon studied with hybrid density functional theory, Appl. Phys. Lett. 103 (5) (2013) 052101, http://dx.doi.org/10.1063/1.4817012.

[41] C. Varvenne, F. Bruneval, M.-C. Marinica, E. Clouet, Point defect modeling in materials: Coupling ab initio and elasticity approaches, Phys. Rev. B 88 (2013) 134102, http://dx.doi.org/10.1103/PhysRevB.88.134102.

[42] H. Wang, A. Chroneos, D. Hall, E.N. Sgourou, U. Schwingenschlögl, Phosphorous–vacancy–oxygen defects in silicon, J. Mater. Chem. A 1 (37) (2013) 11384–11388, http://dx.doi.org/10.1039/C3TA12167D.

[43] L.J. Sham, M. Schluter, Density-functional theory of the band gap, Phys. Rev. B 32 (1985) 3883–3889, http://dx.doi.org/10.1103/PhysRevB.32.3883.

[44] P. Spiewak, K.J. Kurzydłowski, Formation and migration energies of the vacancy in si calculated using the HSE06 range-separated hybrid functional, Phys. Rev. B 88 (19) (2013) 195204, http://dx.doi.org/10.1103/PhysRevB.88.195204, Publisher: American Physical Society.

[45] P. Borlido, J. Schmidt, A.W. Huran, F. Tran, M.A.L. Marques, S. Botti, Exchange-correlation functionals for band gaps of solids: benchmark, reparametrization and machine learning, Npj Comput. Mater. 6 (1) (2020) 1–17, http://dx.doi.org/10.1038/s41524-020-00360-0.

[46] J. Heyd, G.E. Scuseria, M. Ernzerhof, Hybrid functionals based on a screened Coulomb potential, J. Chem. Phys. 118 (18) (2003) 8207–8215, http://dx.doi.org/10.1063/1.1564060.

[47] J. Heyd, G.E. Scuseria, Efficient hybrid density functional calculations in solids: Assessment of the Heyd–Scuseria–Ernzerhof screened Coulomb hybrid functional, J. Chem. Phys. 121 (3) (2004) 1187–1192, http://dx.doi.org/10.1063/1.1760074.

[48] J. Heyd, G.E. Scuseria, M. Ernzerhof, Hybrid functionals based on a screened Coulomb potential, J. Chem. Phys. 118 (18) (2003) 8207–8215, http://dx.doi.org/10.1063/1.1564060.

[49] G. Kresse, J. Furthmüller, Efficient iterative schemes for ab initio total-energy calculations using a plane-wave basis set, Phys. Rev. B 54 (16) (1996) 11169–11186, http://dx.doi.org/10.1103/PhysRevB.54.11169.

[50] G. Kresse, D. Joubert, From ultrasoft pseudopotentials to the projector augmented-wave method, Phys. Rev. B 59 (1999) 1758, http://dx.doi.org/10.1103/PhysRevB.59.1758.

[51] J.P. Perdew, K. Burke, M. Ernzerhof, Generalized gradient approximation made simple, Phys. Rev. Lett. 77 (18) (1996) 3865–3868, http://dx.doi.org/10.1103/PhysRevLett.77.3865.
[52] Y. Okada, Y. Tokumaru, Precise determination of lattice parameter and thermal expansion coefficient of silicon between 300 and 1500 K, J. Appl. Phys. 56 (2) (1984) 314–320, http://dx.doi.org/10.1063/1.333965.
[53] O. Madelung, U. Rössler, M. Schulz, Silicon (Si), Band Structure: datasheet from Landolt-Börnstein - Group III Condensed Matter · Volume 41a1β: "Group IV Elements, IV-IV and III-V Compounds. part B - Electronic, Transport, Optical and Other Properties" in SpringerMaterials, Springer-Verlag Berlin Heidelberg, 2002, http://dx.doi.org/10.1007/10832182_432.
[54] C. Freysoldt, J. Neugebauer, C.G. Van de Walle, Fully Ab initio finite-size corrections for charged-defect supercell calculations, Phys. Rev. Lett. 102 (1) (2009) 016402, http://dx.doi.org/10.1103/PhysRevLett.102.016402.
[55] C. Freysoldt, J. Neugebauer, C.G.V.d. Walle, Electrostatic interactions between charged defects in supercells, Phys. Status Solidi (B) 248 (5) (2011) 1067–1076, http://dx.doi.org/10.1002/pssb.201046289.
[56] W.C. Dunlap, R.L. Watters, Direct measurement of the dielectric constants of silicon and germanium, Phys. Rev. 92 (1953) 1396–1397, http://dx.doi.org/10.1103/PhysRev.92.1396.
[57] C.G. Van de Walle, J. Neugebauer, First-principles calculations for defects and impurities: Applications to III-nitrides, J. Appl. Phys. 95 (8) (2004) 3851–3879, http://dx.doi.org/10.1063/1.1682673.
[58] M.J. Puska, S. Pöykkö, M. Pesola, R.M. Nieminen, Convergence of supercell calculations for point defects in semiconductors: Vacancy in silicon, Phys. Rev. B 58 (3) (1998) 1318–1325, http://dx.doi.org/10.1103/PhysRevB.58.1318.
[59] F. Corsetti, A.A. Mostofi, System-size convergence of point defect properties: The case of the silicon vacancy, Phys. Rev. B 84 (3) (2011) 035209, http://dx.doi.org/10.1103/PhysRevB.84.035209.
[60] A.F. Wright, Density-functional-theory calculations for the silicon vacancy, Phys. Rev. B 74 (16) (2006) 165116, http://dx.doi.org/10.1103/PhysRevB.74.165116.
[61] H. Bracht, H.H. Silvestri, I.D. Sharp, E.E. Haller, Self- and foreign-atom diffusion in semiconductor isotope heterostructures. II. Experimental results for silicon, Phys. Rev. B 75 (2007) 035211, http://dx.doi.org/10.1103/PhysRevB.75.035211.
[62] A.O. Evwaraye, E. Sun, Electron irradiation induced divacancy in lightly doped silicon, J. Appl. Phys. 47 (9) (1976) 3776–3780, http://dx.doi.org/10.1063/1.323260.
[63] A.N. Larsen, A. Mesli, K. Bonde Nielsen, H.K. Nielsen, L. Dobaczewski, J. Adey, R. Jones, D.W. Palmer, P.R. Briddon, S. Öberg, E center in silicon has a donor level in the band gap, Phys. Rev. Lett. 97 (10) (2006) 106402, http://dx.doi.org/10.1103/PhysRevLett.97.106402, Publisher: American Physical Society.
[64] M. Lannoo, Evidence for correlation effects in the hyperfine structure of the negative vacancy in silicon, Phys. Rev. B 28 (5) (1983) 2403–2410, http://dx.doi.org/10.1103/PhysRevB.28.2403.
[65] M. Sprenger, S.H. Muller, E.G. Sieverts, C.A.J. Ammerlaan, Vacancy in silicon: Hyperfine interactions from electron-nuclear double resonance measurements, Phys. Rev. B 35 (4) (1987) 1566–1581, http://dx.doi.org/10.1103/PhysRevB.35.1566.
[66] J.W. Corbett, G.D. Watkins, Silicon divacancy and its direct production by electron irradiation, Phys. Rev. Lett. 7 (1961) 314–316, http://dx.doi.org/10.1103/PhysRevLett.7.314.
[67] G.A. Baraff, E.O. Kane, M. Schlüter, Theory of the silicon vacancy: An Anderson negative-U system, Phys. Rev. B 21 (12) (1980) 5662–5686, http://dx.doi.org/10.1103/PhysRevB.21.5662.
[68] G.D. Watkins, J.R. Troxell, Negative-U properties for point defects in silicon, Phys. Rev. Lett. 44 (9) (1980) 593–596, http://dx.doi.org/10.1103/PhysRevLett.44.593.
[69] J. Mäkinen, C. Corbel, P. Hautojärvi, P. Moser, F. Pierre, Positron trapping at vacancies in electron-irradiated Si at low temperatures, Phys. Rev. B 39 (1989) 10162–10173, http://dx.doi.org/10.1103/PhysRevB.39.10162.
[70] V.V. Lukjanitsa, Energy levels of vacancies and interstitial atoms in the band gap of silicon, Semiconductors 37 (4) (2003) 404–413, http://dx.doi.org/10.1134/1.1568459.
[71] D.R. Bosomworth, W. Hayes, A.R.L. Spray, G.D. Watkins, B. Bleaney, Absorption of oxygen in silicon in the near and the far infrared, Proc. R. Soc. Lond. Ser. A Math. Phys. Eng. Sci. 317 (1528) (1970) 133–152, http://dx.doi.org/10.1098/rspa.1970.0107.
[72] J.W. Corbett, R.S. McDonald, G.D. Watkins, The configuration and diffusion of isolated oxygen in silicon and germanium, J. Phys. Chem. Solids 25 (8) (1964) 873–879, http://dx.doi.org/10.1016/0022-3697(64)90100-3.
[73] B. Pajot, in: R. Willardson, A.C. Beer, E.R. Weber (Eds.), Chapter 6 Some Atomic Configurations of Oxygen, in: Semiconductors and Semimetals, vol. 42, Elsevier, 1994, pp. 191–249, http://dx.doi.org/10.1016/S0080-8784(08)60249-5.
[74] E.L. Elkin, G.D. Watkins, Defects in irradiated silicon: Electron paramagnetic resonance and electron-nuclear double resonance of the arsenic- and antimony-vacancy pairs, Phys. Rev. 174 (3) (1968) 881–897, http://dx.doi.org/10.1103/PhysRev.174.881.
[75] G.D. Watkins, Understanding the Jahn–Teller distortions for the divacancy and the vacancy–group-V-atom pair in silicon, Physica B 376–377 (2006) 50–53, http://dx.doi.org/10.1016/j.physb.2005.12.014.
[76] D. Mathiot, J.C. Pfister, Dopant diffusion in silicon: A consistent view involving nonequilibrium defects, J. Appl. Phys. 55 (10) (1984) 3518–3530, http://dx.doi.org/10.1063/1.332941.
[77] H. Park, M.E. Law, Point defect based modeling of low dose silicon implant damage and oxidation effects on phosphorus and boron diffusion in silicon, J. Appl. Phys. 72 (8) (1992) 3431–3439, http://dx.doi.org/10.1063/1.351416.
[78] B. Baccus, T. Wada, N. Shigyo, M. Norishima, H. Nakajima, K. Inou, T. Iinuma, H. Iwai, A study of nonequilibrium diffusion modeling-applications to rapid thermal annealing and advanced bipolar technologies, IEEE Trans. Electron Devices 39 (3) (1992) 648–661, http://dx.doi.org/10.1109/16.123491.